Journal of Electronic Materials, Vol. 4, No. 1, 1975

THE ROLE OF IONIZATION COEFFICIENT IN THE OPERATION OF AVALANCHE DIODES ABOVE BREAKDOWN

P. Antognetti

Istituto di Elettrotecnica
Università di Genova
Viale Cambiaso 6 - 16145 Genova, Italy

W. G. Oldham

Department of Electrical Engineering and Computer Sciences
and the Electronics Research Laboratory
University of California, Berkeley, California 94720

(Received September 9, 1974; revised November 5, 1974)

The behavior of the avalanche triggering probability in pn junction diodes biased above breakdown is a sensitive function of the form of the field dependence of α_e and α_h. In this paper we present theoretical predictions of electron and hole initiated avalanche triggering probabilities in planar, cylindrical, and spherical junctions. These probabilities are calculated as a function of excess bias above breakdown for various forms of α_e and α_h versus E. We also show recent experimental data for electron and hole triggering in planar diodes. The absolute electron triggering probability is measured to an accuracy of about $\pm$ 40%. The form of the

Work supported in part by Consiglio Nazionale delle Ricerche (CNR), Italy, and in part by the Joint Services Electronics Program, Contract F-44620-71-C-0087.

© 1975 by the American Institute of Mining, Metallurgical, and Petroleum Engineers, Inc. No part of this publication may be reproduced, stored in a retrieval system, or transmitted, in any form or by any means, electronic, mechanical, photocopying, microfilming, recording, or otherwise, without written permission of the publisher.

electron and hole triggering probabilities versus bias are more accurately determined. Both the absolute and relative triggering probabilities are in good agreement with the theoretical prediction based on α_e and α_h forms of either Grant or Van Overstraeten and De Man.

Key words: ionization coefficients, avalanche triggering probabilities.

Introduction

The knowledge of the ionization coefficients is important in predicting the behavior of avalanche devices, as illustrated for example by the IMPATT diode calculations of Seddik and Haddad. They show a strong dependence of IMPATT diode parameters on the form of the ionization coefficients (1). Several recent experimental studies of multiplication in pn junctions yield values and forms of the field dependence of the ionization coefficients (2,3) different from the commonly accepted "standard" values (4,5). The most recent data of Grant (3) are in general agreement with the Van Overstraeten and De Man results (2), except for an overall 20–30% increase in α_e and α_h.

The operation of avalanche diodes above the breakdown voltage has been explored experimentally, and their use as detectors and noise sources has been suggested (6–11).

Recently, two differential equations have been developed for the triggering probability, the probability that a free carrier in transit in the depletion region initiates a self sustaining avalanche (12). The equations were solved numerica ly for a n^+p planar diode, and the results compared with experiments on special "miniature avalanche diode" structures The general form of the triggering probability versus excess bias was verified, both for electrons and holes. The behavior of the avalanche triggering probability in such diodes is als a sensitive function of the form of the field dependence of α_e and α_h (12).

In this paper we extend the solutions of the triggering probability to cylindrical and spherical step junctions and to p-i-n diodes. These probabilities are calculated as a function of excess bias above breakdown for various forms of α_e and α_h versus E. We also show recent experimental data for electron and hole triggering in planar diodes. The absolute electron triggering probability is measured to an accuracy of about $\pm$ 40%. Both the absolute and relative triggering probabilities versus bias are in good agreement with the theoretical prediction based on α_e and α_h forms of either Grant (3) or Van Overstraeten and De Man (2). We also derive analytic solutions for the triggering probabilities for the case the ratio of the electron to hole ionization coefficient is a constant and use these results to determine the voltage dependence of the triggering probabilities near breakdown for p-i-n diodes.

Triggering probabilities for planar, cylindrical and spherical junctions.

We consider a planar uniform avalanche diode biased above breakdown with no current flowing. In all numerical calculations an n^+p abrupt junction is assumed with x = 0 taken at the n^+ edge, and with x = W taken at the p edge of the space-charge region. It can be shown (12) that the probability $P_e(x)$ that an avalanche will be initiated by an electron which has been generated at position x in the depletion region can be calculated exactly from the set of differential equations

$$dP_e / dx = (1-P_e)\, \alpha_e (P_e + P_h - P_e P_h) \quad (1)$$

$$dP_h / dx = -\, (1-P_h)\, \alpha_h (P_e + P_h - P_e P_h) \quad (2)$$

where $P_h(x)$ is the probability for initiation of an avalanche by a hole generated at x, and $\alpha_e(x)$, $\alpha_h(x)$ are

the electron and hole ionization rates, respectively. The two boundary conditions necessary for integrating (1) and (2) are

$$P_e(0) = 0 \tag{3}$$

$$P_h(W) = 0 \tag{4}$$

In Eqs. (1) and (2) the variable may be transformed from distance to electric field, since this is the physical parameter on which the ionization rates depend. In the case of an abrupt junction, the x-dependence of E is derived from Poisson's equation

$$E(r) = -\frac{qN_B}{\varepsilon r^n} \int_{r_j}^{r} r^n \, d\, r + \frac{A}{r^n} \tag{5}$$

where n is equal to 0 for the planar case, to 1 for the cylindrical junction and to 2 for the spherical junction, and A is a constant of integration; its value is determined by setting $E(r_j+W) = 0$ and

requiring $\int_{r_j}^{r_j+W} E\, dr = V$, the applied voltage; r_j is the radius of curvature of the junction.

Numerical solutions for Eqs. (1) and (2) have been obtained by using the following method. At the n^+ edge of the space-charge region, P_e is set to zero [boundary condition Eq. (3)] and P_h is assigned some value in the range 0 to 1. A guess is made for the value of V (some value $V > V_B$) and corresponding values for E(x) and $\alpha(x)$ are

determined from Eq. (5) and the known ionization coefficients. Eqs. (1) and (2) are integrated simultaneously to $E = 0$, at $r = r_j + W$, and thus P_h at the p-edge of the space-charge region is determined. The voltage V is then varied iteratively until boundary condition Eq. (4) is satisfied. This algorithm is repeated for different initial values of $P_h(E_{max})$ at the n^+-edge of the space-charge region, yielding the voltage dependence of P_e and P_h throughout the space-charge region. The breakdown voltage, V_B, is also determined by finding the voltage for which $P_h(E_{max}) \rightarrow 0$. This procedure for determining V_B essentially simulates the experimental method suggested in (11), and is equivalent to the evaluation of the standard breakdown integral (5).

An important role is played by the field-dependence of the ionization coefficients. We have considered recent data from the literature (2,3) and found them essentially equivalent for our purposes, e.g., for an n^+-p step junction with $N_A = 3 \times 10^{16}$ cm^{-3} the triggering probabilities calculated using Grant's ionization coefficients (3) are nearly identical with the probabilities computed using the ionization data by Van Overstraeten and De Man (2), with only a 25% increase in doping. In all the numerical calculations we have used functions $\alpha_{e,h}(E)$ for silicon fitting the experimental data by Van Overstraeten and De Man (2).

The form of $P_e(x)$ and $P_h(x)$ for a specific case has been shown previously (12). Here we display only the limiting values, $P_h(0)$ and $P_e(W)$, i.e., the probability that a hole or an electron in traversing the entire depletion layer triggers an avalanche. These probabilities are sketched as a function of excess bias above breakdown in Fig. 1, for an n^+-p planar junction with background doping

$N_B = 3 \times 10^{16}\ cm^{-3}$. It is seen that close to breakdown the triggering probabilities are proportional to the excess bias. The experimental points shown in Fig. 1 were taken with n^+p uniform avalanche diodes, constructed according to Ref.(12), illuminated with light at two different wave-lengths in order to have pure hole or pure electron avalanche triggering; the experimental pulse rates were normalized at 3.4 V to the theoretical triggering probabilities, because an accurate absolute measurement of the triggering probabilities is difficult (see later section). The results shown in Fig. 1 are in much better agreement with theory than was the case in the analogous figure (Fig. 5) in Ref. (12). The difference lies in the field-dependence of the ionization coefficients used in the numerical calculations; in Ref. (12) functions fitting the data by Lee et al. (4) were used. It is also interesting to note that the newer ionization coefficients yield a theoretical breakdown voltage in excellent agreement with experiments in this work.

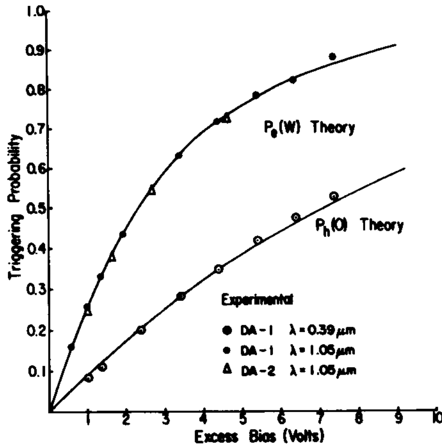

Fig. 1. $P_e(W)$ and $P_h(0)$ for an n^+p junction with substrate doping $3 \times 10^{16}\ cm^{-3}$.

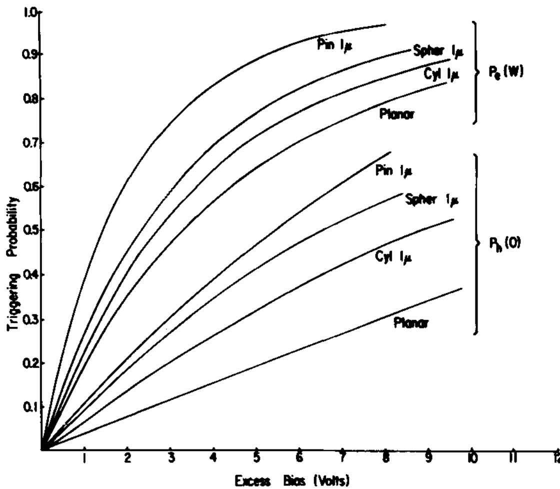

Fig. 2. $P_e(W)$ and $P_h(O)$ for planar, cylindrical (radius 1μm), spherical (radius 1 μm) n^+p junctions with substrate doping 1×10^{16} cm^{-3}, and for p-i-n diode with 1 μm i-region width.

Fig. 2 shows similar curves to Fig. 1 for various junction geometries of possible use, for example in avalanche photodiodes (9). The triggering probabilities for carriers transiting the entire depletion region are plotted as a function of excess bias, for an assumed substrate doping $N_B = 10^{16}$ cm^{-3}. A 1 μm radius of curvature is assumed for the spherical and cylindrical junctions. Also shown for comparison are the analogous rates for a p-i-n diode with 1 μm i-region width. The p-i-n curves are constructed from an anlytical solution of Eqs. (1) and (2), discussed in the next section.

The triggering probability curves for various dopings and radii are all similar in shape, if normalized to a common initial slope. Therefore, we can present most of the information in the P_e and P_h plots by merely stating the slopes dP_e / dV and dP_h / dV near zero excess voltage.

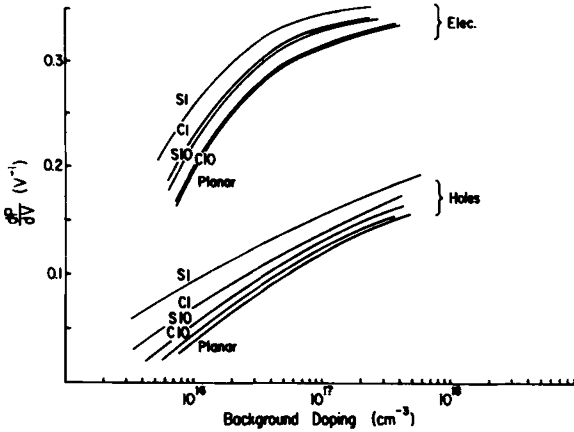

Fig. 3. Initial slope dP/dV for electrons and holes versus substrate doping for planar, cylindrical (1 and 10 μm radius; C1 - C10) and spherical (1 and 10 μm radius; S1 - S10) junctions.

Fig. 3 shows the doping dependence of the dP/dV curves for the planar, cylindrical and spherical junctions.

Analytic treatment for the case $\vartheta = \alpha_e / \alpha_h$ = const.

If the ratio of the ionization coefficients is constant, Eqs. (1) and (2) may be integrated to yield closed form implicit expressions for P_e and P_h. McIntyre (13) has derived an effective ratio which allows, in principle, the use of these expressions even if ϑ is not constant. We outline here a simple method for obtaining P_e and P_h.

We first define the quantities $P'_e = 1 - P_e$, $P'_h = 1 - P_h$.

Dividing equation (1) by (2) and integrating from 0 to x we obtain

$$\ln P'_e(x) = \vartheta \ln P'_h(0) / P'_h(x) \qquad (6)$$

where we have used boundary condition Eq. (3).

Thus the triggering probabilities at the boundaries, $P_e(W)$, $P_h(0)$ are related by

$$P'_e(W) = P'_h(0)^{\vartheta} \tag{7}$$

Eq. (6) may be substituted into Eq. (2) which then can be integrated to yield

$$\frac{\left[P'_h(x)/P'_h(0)\right]^{\vartheta-1} - P'_h(0)}{1 - P'_h(0)} = \exp(\vartheta-1)\int_0^x \alpha_h \, dx \tag{8}$$

and $P_e(x)$ may be obtained from Eq. (6).

In addition to their application in non-Si materials, these equations may be used to evaluate P_e, P_h in Si p-i-n diodes. The breakdown voltage is obtained from the usual breakdown integral, and Eq. (8) is solved at various voltages above this value.

In materials with $\alpha_e / \alpha_h = 1$, Eq. (8) has a trivial solution. However, the limit for $\vartheta \rightarrow 1$ yields the correct form in this case:

$$P'_h(x) = P'_h(0) \exp\left[1 - P'_h(0)\right]\int_0^x \alpha \quad dx \tag{9}$$

The curves labeled 'pin' in Fig. 2 were computed using Eqs. (7) and (8) evaluated at x = W = 1 μm.

Experiments on planar junctions

We have measured the absolute triggering rate of the diode of Fig. 1 under conditions of known illumination intensity, and compared the measurements with a theoretical prediction, in a further attempt to distinguish between different ionization rates characterizations. If the junction is illuminated with penetrating light ($\lambda \approx 1.1\ \mu m$), only electron triggering is significant. Electrons diffusing from the neutral p-region (Fig. 4) have a triggering probability $P_e(W)$ for a given excess bias, as shown in Fig. 1. Electrons generated within the space-charge region (active region) have an average probability of $0.8 \times P_e(W)$ of triggering an avalanche at 1V above the breakdown voltage (cfr. Fig. 4, Ref. 12).

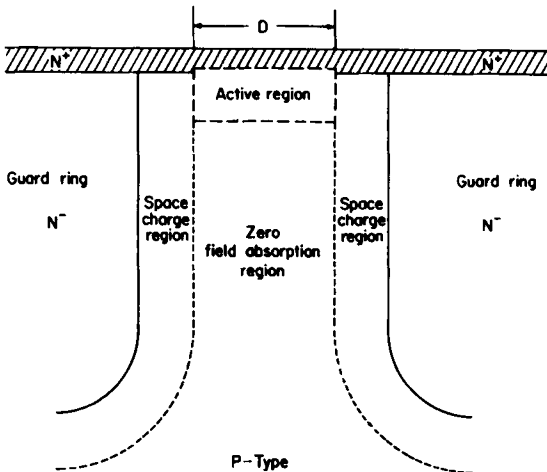

Fig. 4. Schematic cross-section of the active region of the uniform avalanche diode.

The diodes were illuminated with monochromatic light at various wavelengths from 1.05 to 1.12 μm. The illumination intensity F was measured with an HP 8330 radiant flux meter. The absorption coefficient α was measured at each wavelength using silicon slabs of different thickness, taking into account multiple reflections. Thus the volume generation rate was determined, directly at the sample temperature, as $F\alpha / h\nu$.

The knowledge of the active volume of the device allows the determination of the absolute triggering probability from the measured pulse-rate. However the exact determination of the active volume (Fig. 4) is rather difficult. We first determine the diameter D of the active region and then compute the active volume from D. The effective active volume consists of the space-charge region volume x 0.8 plus an effective volume corresponding to collection from the neutral p-type bulk. The latter may be calculated from diffusion theory.

The diameter D may be estimated in two ways, from the total apparent series resistance, and from a scanning light spot measurement. For the particular diode used in these experiments, the series resistance at 23°C was 3.1 KΩ. This value is the sum of three terms, the spreading resistance, the space-charge resistance, and the thermal resistance (14). Since these components differ in their dependance on diameter, a unique diameter may be selected which yields the measured total resistance. However, the length of the zero-field absorption region (Fig. 4) is not known exactly because of the particular geometry of the diode; thus we can only determine $D = 6\mu \pm 1\mu$ from the resistance measurement. An alternative measurement used a scanning submicron light spot to estimate D. The pulse rate was measured as the spot was scanned across the junction. (In the course of this experiment we observed that the breakdown voltage was independent of light spot position. This is somewhat unexpected based on the large variations predicted by Shockley (15)). The half width of the response

at $\lambda = 10{,}000$ Å is 7 μm, and at 8,000 Å, 4.3 μm. Such large difference presumably arises from the complicated collection probability function. We can only conclude that a diameter of 6 μm is not inconsistent with the light probe measurement.

The effective active volume for pure electron triggering was computed from diffusion theory. The flux $\mathcal{F}$ of carriers into the end of a cylinder with infinite recombination at the side walls is analogous to the cylindrical heat flow problem with constant side wall temperature and uniform heat generation (16). The effective collection volume is defined as the volume in which $\mathcal{F} \cdot \pi D^2/4$ carriers are generated (uniform generation rate). We obtain a volume of 2.7×10^{-11} cm^3 for D = 6 μm. This value is very sensitive to D; it varies from 1.6 to 4.3×10^{-11} cm^3 as D goes from 5 to 7 μm. In addition, the space-charge region effective volume equals 2.2×10^{11} cm^3 for D = 6 μm, and varies from 7.6 to 3.1×10^{-11} cm^3 as D goes from 5 μm to 7 μm. Thus the total effective volume figures are 3.2 4.9, and 7.4×10^{-11} cm^3 for D = 5, 6, and 7 μm, respectively.

The effective volume was determined experimentally by dividing the measured pulse rate by the triggering probability $P_e(W)$ (corresponding to that excess bias, Fig. 1) and the generation rate (as discussed above). For the diode of Fig. 1, we determine an effective volume of $2.5 \pm .2$ x x 10^{-11} cm^3. If, instead of Van Overstraeten and De Man's ionization rates curves, the form given by Sze (5) is used, the effective volume is reduced to $\sim 1.4 \times 10^{-11}$ cm^3 because of the increased triggering probability at 1 V excess bias (see Fig. 5, Ref. 12).

Both of these values are smaller than the theoretically predicted effective volume of 4.9×10^{-11} cm^3 for D = 6 μm. A value of D = 4.6 μm is required to predict a volume of

2.5×10^{-11} cm^3, and an even smaller value of 3.2 μm would yield an effective collection volume of 1.4×10^{-11} cm^3. The former, while slightly outside the confidence range of our diameter measurement is possible, the latter is not. Thus the absolute triggering rate measurement is also consistent with the more recent ionization rate measurements (2,3).

Acknowledgement

The authors gratefully acknowledge the assistance of W. W. Yen Chu in performing the light probe experiment.

References

(1) M. M. Seddik and G. I. Haddad, IEEE Trans. El. Dev., ED-20, 1164 (1973).

(2) R. Van Overstraeten and H. De Man, Solid State Electron., 13, 583 (1970).

(3) W. N. Grant, Solid State Electron., 16, 1189 (1973).

(4) C. A. Lee, R. A. Logan, R. L. Batdorf, J. J. Kleinack and W. Wiegmann, Phys. Rev., 134, A761 (1964); J. L. Moll and R. Van Overstraeten, Solid State Electron., 6, 147 (1963).

(5) S. M. Sze, Physics of Semiconductor Devices, Wiley, New York (1969).

(6) G. Keil, H. Bernt, Solid State Electron., 9, 321 (1966).

(7) R. H. Haitz, IEEE Trans. Elec. Dev., ED-13, 342 (1966).

(8) R. H. Haitz and F. W. Voltmer, Jour. Appl. Phys. 39, 3379 (1968).

(9) H. Sigmund, Infrared Phys., 8, 259 (1968).

(10) P. P. Webb and R. J. McIntyre, Bull. Amer. Phys. Soc. II, 15, 813 (1970).

(11) W. G. Oldham, P. Antognetti and R. R. Samuelson, Appl. Phys. Lett., 19, 466 (1971).

(12) W. G. Oldham, R. R. Samuelson and P. Antognetti, IEEE Trans. Elec. Dev., ED-19, 1056 (1972).

(13) R. J. McIntyre, IEEE Trans. Elec. Dev., ED-20, 637 (1973).

(14) R. H. Haitz, H. L. Stover and N. J. Tolar, IEEE Trans. El. Dev., ED-16, 438 (1969).

(15) W. Shockley, Solid State Electron., 2, 35 (1961).

(16) H. S. Carslaw and J. C. Jaeger, Conduction of Heat in Solids, Clarendon Press, Oxford (1959).